CHALMERS
UNIVERSITY OF TECHNOLOGY

Risk analysis methodology for ship-bridge allisions – A combined probability and consequence analysis

Engineering Structures 347 (2026) 121731

Contents lists available at ScienceDirect

Engineering Structures

journal homepage: www.elsevier.com/locate/engstruct

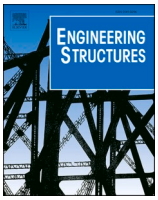

Risk analysis methodology for ship-bridge allisions – A combined probability and consequence analysis

Axel Hörteborn [a,b,*], Yanyan Sha [c], Jonas W. Ringsberg [b], Olov Lundbäck [a], Wengang Mao [b]

[a] RISE, Research Institutes of Sweden, Safety and Transport, Maritime Department, Gothenburg SE-412 58, Sweden
[b] Chalmers University of Technology, Department of Mechanics and Maritime Sciences, Division of Marine Technology, Gothenburg SE-412 96, Sweden
[c] Department of Mechanical and Structural Engineering and Materials Science, University of Stavanger, Stavanger 4036, Norway

ARTICLE INFO

Keywords:
Automatic identification system data
Maritime risk analysis
Allisions
Monte Carlo simulations

ABSTRACT

Ship-bridge allision risk assessments often address either probability or consequence; integrations of both in a unified methodology are rare. This paper fills that gap by introducing Ship Traffic Allision Probability using Monte Carlo Simulations – consequence (STAPS-cons), a methodology where a mid-fidelity simulation methodology developed for probability assessment is used together with the results of Finite Element Analysis (FEA) simulations to include consequence assessments. Using Automatic Information System (AIS) data and the proposed methodology, a potential bridge over Norway's Bjørnafjorden is analysed in a case study to determine the risk of structural collapse. The case study also illustrates how the risk is affected by different input parameters, both related to probability and consequence estimations. Five scenarios were analysed in this case study; three passed and two failed the Norwegian criterion for the probability of structural collapse, which is less frequent than 10^{-4} per year. A 20 % increase in the duration of a ship's miss of turning point notably raised both the allision frequencies and the necessary levels of energy the bridge must withstand. In another scenario, where a less stiff bridge structure was analysed, the demand on the global structure decreased. In conclusion, the STAPS-cons methodology represents a significant advancement in the field of ship-bridge allision risk assessment. By integrating probability and consequence assessments, this methodology offers a more robust and comprehensive tool for managing the risks associated with increased shipping traffic and bridge construction in navigational waters.

1. Introduction

With the increasing ship traffic worldwide and the constant increase in ship size, the risks of ship-bridge allisions in navigational waters have become increasingly imperative. The preferred terminology in this context is 'allision' to describe ships hitting stationary structures, as opposed to ship-ship collision. There are challenges that need to be considered with regards to different design perspectives, such as the design of new bridges, the design and allision resistance of existing bridges and how shipping traffic fairways should be designed to avoid ship-bridge allisions.

The March 2024 accident involving the DALI ship striking the Francis Scott Key Bridge in Baltimore (USA) [1] exemplifies the potentially grave ramifications of a ship-bridge allision, with fatalities, significant environmental damage and enormous societal costs that will affect Baltimore for decades. According to Zhang et al. [2] there were at least 29 ship-bridge allisions with severe consequences between the 1 January 2018 and the 1 April 2024. Most of these bridges had already considered ship allision scenarios at the time of their design and construction, given the statistics of ship traffic, sizes, and tonnages at that time. However, since the progression in ship transportation has advanced faster than the bridges' original construction was designed to encounter these statistics have become outdated [3].

The current study addresses the need both to continuously revisit old bridge designs in the context of changing ship traffic and have a proactive mitigation mindset in future changes to the waterways, considering ship traffic as well as environmental and societal safety. It is of the utmost importance that both new bridge designs (stationary or floating) and existing bridges learn from incidents and accidents so that risks can be proactively minimised. Today, two principal bridge-building codes

* Corresponding author at: RISE, Research Institutes of Sweden, Safety and Transport, Maritime Department, Gothenburg SE-412 58, Sweden.
E-mail address: axel.horteborn@ri.se (A. Hörteborn).

https://doi.org/10.1016/j.engstruct.2025.121731
Received 5 June 2025; Received in revised form 16 October 2025; Accepted 7 November 2025
Available online 18 November 2025

are employed for this purpose: American Association of State Highway and Transportation Officials (AASHTO) [4] and the Eurocode [5]. As AASHTO was adopted in 1991, it recommends that a vulnerability analysis should be conducted on bridges that were built prior to this standard being enforced. AASHTO uses two acceptance criteria with regards to structural collapses: an annual probability of less than (i) 10^{-3} for regular bridges and (ii) 10^{-4} for critical bridges. The Eurocode states that risk acceptance criteria should be defined in local annexes, which, in Norway, is defined as, 'The occurrence and consequence of accidental loads usually related to a certain risk level. To the extent the accidental load can be determined by probability calculations, the probability of events that can be disregarded in the analysis shall not exceed 10^{-4} per year' [6]. Many scholars have studied marine traffic probability assessments of ship-bridge allisions. The works presented in [7–9] highlight that probability assessments in most existing methodologies are refinements of Fujii et al. [10] and Macduff [11] from the 1970s. Pedersen [12] further refined the probability assessment framework to ease probability calculations and assessments. Based on this work, Friis-Hansen [13] established the IWRAP Mk II software [14], which is recommended by the International Maritime Organisation (IMO) [15] for quantitative probability assessments of maritime accidents. This software is used to quickly determine a rough estimate of the probability of ship-bridge allisions. It should be noted that it cannot consider the ship's hydrodynamics, which, in accident scenarios, can be a significant factor. Nevertheless, the software is considered a good tool for engineers since its computation time is low, and few parameters are needed to analyse various scenarios. To overcome the lack of ship hydrodynamics in the probabilistic assessment, Bąk et al. [16] proposed the use of ship manoeuvre simulators to improve the realism of accident scenario modelling. Similarly, Hörteborn et al. [17] developed the Ship Traffic Allision Probability using Monte Carlo Simulations (STAPS) methodology, which integrates vessel-specific manoeuvrability and environmental conditions through a maritime manoeuvre simulator (MMS). In a comparative study, STAPS was benchmarked against IWRAP Mk II, demonstrating that the latter tends to overestimate accident probabilities due to simplified failure modelling and static drift assumptions.

Consequence analyses for ship-ship collisions and ship-bridge allisions are often studied using different approaches via specific events or scenarios. Minorsky [18], one of the pioneers in the field, analysed ship-ship collisions to determine safety standards for protecting nuclear power plants. The study found that the deformed volume of the ships was related to their kinetic energy. Since the studies by Minorsky, multiple analytical and semi-analytical methods for structural integrity and crashworthiness consequence analyses have been developed. Most studies in the literature use nonlinear Finite Element Analyses (FEA) because of complex hydro-mechanical coupling effects and a need to resolve energy distribution and dissipation into different parts of the structures involved in the simulation.

Le Sourne et al. [19] proposed the MCOL tool in LS-DYNA software, which combines the consideration of internal mechanics and external dynamics. It enables a detailed assessment of structural integrity consequences, considering hydrodynamic-mechanical couplings in a realistic physics setting. This advantage of high-resolution, detailed information comes with the cost of extensive computational efforts; hence, it is suitable for a few scenario simulations. Sha et al. [20] simulated ship-bridge allisions of a sizeable floating bridge across a Norwegian fjord. They divided their simulations into local structural damages using LS-DYNA and global dynamic responses of the bridge using USFOS software. A parameter sensitivity analysis showed the bridge's response to various allision scenarios, which were defined without any connection to their probability of occurrence. Barge-bridge allisions were studied by Chen et al. [21] using FEA. The purpose was to simulate and analyse bridge resistance to barge allisions and to propose mitigation actions based on numerical simulations and the Taiyangbu Bridge (China) bridge allision accident. Lu et al. [22] used centrifuge modelling to study progressive collapse in a multi-span bridge. They found that as much as 40 % of the kinetic energy from the ship could be transferred to the bridge-soil system. Wang et al. [23] used OrcaFlex software to simulate and analyse ship-bridge allisions under the influence of winds and waves. The authors studied the global response of a floating bridge, considering loads from waves and wind, and ship allision cases (ship type, kinetic energy, allision location, etc.). It was concluded that including wind and wave loads influences the results, with the allision location and angle of attack being sensitive parameters in the simulation model as well.

While many scholars continue to present methods for estimating the consequence of ship-bridge allisions using nonlinear FEA, the studies presented in [12,24–29] show the possibility of combining analytical methods, semi-analytical methods and FEA in collision analyses involving ships. Some of these studies also showed that simplified analytical expressions that apply energy dissipation internally in structures during ship-collision events can be used, as they often match experimental results and nonlinear FEA.

There are examples of risk assessment methodologies that focus on probability or consequence, but few include both aspects in the same methodology. The works in [12,27,30,31] present probability and consequence analyses, strongly emphasising the need for one integrated methodology to simulate and analyse different consequences and their probabilities in risk assessments. The objective of the current study is to present such a methodology and its components. The proposed methodology, Ship Traffic Allision Probability using Monte Carlo Simulations – consequence (STAPS-cons), has been developed to meet the demands for better risk assessment methodology to re-evaluate existing bridge designs and the structural safety of new bridges against ship-bridge allisions, considering current and future accident scenarios. The novelty of the methodology lies in the combination of a mid-fidelity model called STAPS developed by the authors in previous work [17] for accident probability calculations, with a newly developed consequence model that employs consequence analysis based on nonlinear FE model developed by Sha et al. [20]. In this study, the STAPS-cons methodology is applied to a vase study of a ship-bridge allision for a floating bridge.

The remainder of the paper is organised as follows: Chapter 2 presents a brief overview of the STAPS methodology and the components that have been added to form STAPS-cons. Chapter 3 presents a case study of a floating bridge struck by a ship in different scenarios. The results from the case study are presented in Chapter 4, followed by a discussion in Chapter 5 on how the STAPS-cons methodology can be applied for mitigation action analyses, improvements in bridge designs and marine traffic planning. Finally, in Chapter 6, the conclusions of the study are presented.

2. Methodology

In this chapter, Section 2.1 presents the new STAPS-cons methodology, which is based on the STAPS methodology presented in detail in Hörteborn et al. [17]. Section 2.2 introduces the new module that has been added to incorporate consequence assessments in STAPS-cons regarding the structural integrity of damaged structures. The novelty in this paper lies in the transition from a probabilistic methodology to a risk methodology, where the consequence estimation is added to the STAPS methodology. Fig. 1 shows a flowchart of the STAPS-cons methodology, where the green boxes represent the additional consequence module to the former STAPS methodology.

A limited number of 'FE analyses' are conducted with a specific ship hitting a specific bridge. These cases are used in the 'consequence analysis', where they are combined with the output from the Maritime Manoeuvre Simulator (MMS) to estimate the consequence of each allision. This combined output will determine if enough kinetic energy is transferred to the bridge for it to collapse, thereby allowing the risk of collapse to be estimated. Section 2.2 presents the details of how the forces are estimated in the new consequence module added to STAPS, forming the STAPS-cons methodology.

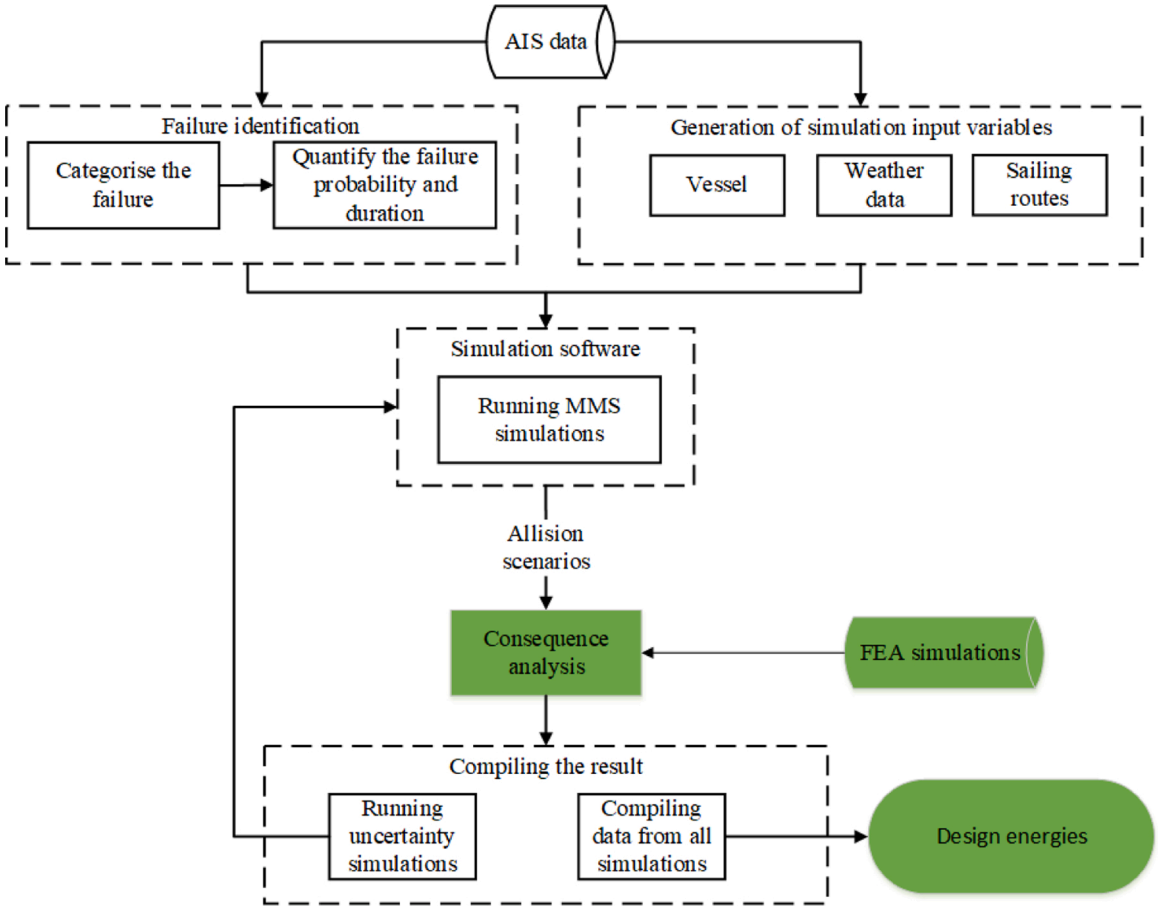

Fig. 1. The STAPS-cons methodology overview. The green boxes are the main contribution in this paper, differentiating the STAPS and STAPS-cons methodologies.

2.1. Probabilistic simulations

The STAPS model is a mid-fidelity model for ship traffic allision probability estimation, which includes a ship's manoeuvrability and motion physics, using the Monte Carlo simulation method for probabilistic calculations. Its origin and details are described in detail in Hörteborn and Ringsberg [32], followed by an extension in Hörteborn and Eidem [33], where active navigational errors can be included in a simulation. One novelty of STAPS is its inclusion of detailed local failure statistics of ship traffic scenarios, which are important in tailoring risk assessments to local areas. The STAPS model in [17], which is used in the current study, can simulate five failure types that may result in a ship-allision accident: loss of propulsion, loss of steering, miss of turning point, wrong course at a turning point (WCT) and turn at the wrong location (TWL); see Fig. 2. Each failure type has a predetermined routine that reduces the model's autopilot's ability to navigate the ship according to the predefined routes.

AIS data are used to identify normal operations in a specific geographic area and to determine the probability and duration of failures. The ship's manoeuvrability and motion physics are handled by a maritime manoeuvre simulator (MMS). STAPS uses Seaman [34,35] as its MMS. Seaman is a modular simulation tool where force-generating

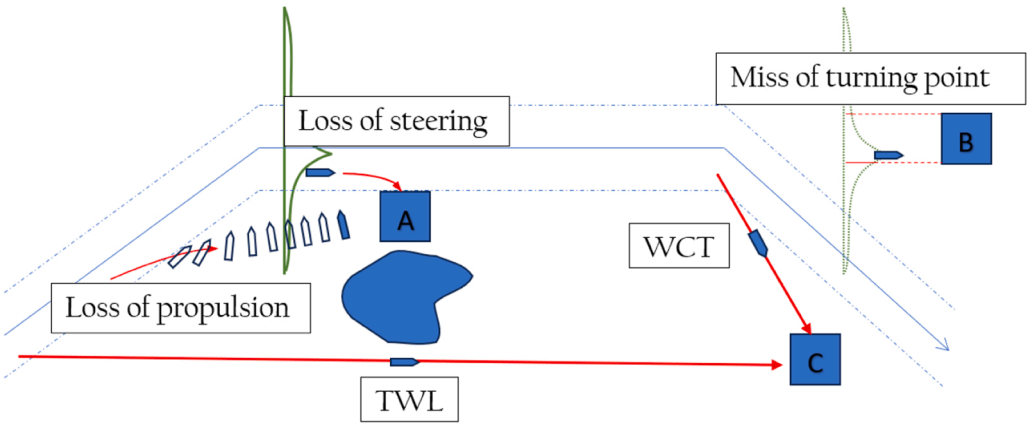

Fig. 2. Examples of a sailing fairway, passing one island and three structures (A, B and C). Paths of the five failure types are included to illustrate how each could result in an allision.

systems are connected to one ship object, which uses PySim [36] to solve the equations for seakeeping motions and manoeuvrability characteristics. Each ship has a unique hydrodynamic specification to be used in the MMS that defines the ship's manoeuvrability characteristics. The Seaman MMS can simulate ships either in full mission, with screens surrounding in 360 °, or in a desktop environment with a single computer. The simulations can be carried out in real-time or fast-time mode in the desktop environment. STAPS uses the fast-time mode, where one fast-time simulation of a 15-minute ship route takes approximately 1 s to run. A ship is simulated using an autopilot, first without failures to ensure that the ship can follow the intended route in all weather conditions, and thereafter with 'triggers' to the aforementioned failure types; see Hörteborn et al. [17] and Hörteborn and Ringsberg [32] for details.

The estimation of the allision probability in STAPS requires millions of simulations to be executed in an MMS simulator. These simulations are executed in sets with the same *failure type* (ft), *route* (r) and *ship category* (sc). The number of simulations to run in each set for the failure types *loss of propulsion*, *loss of steering* and *TWL*, $N^{\text{sim}}_{\text{ft,r,sc}}$, is estimated by Eq. (1). The number of simulations to run for the failures that occur at planned turns (*miss of turning point* and *WCT)*, $M^{\text{sim}}_{\text{ft,r,sc}}$, is estimated by Eq. (2).

$$N^{\text{sim}}_{\text{ft,r,sc}} = N_{\text{r,sc}} \times P_{\text{fte}} \times \left(\frac{L_{\text{r}}}{v_{\text{sc}}}\right) \times Y_{\text{rep}} \tag{1}$$

$$M^{\text{sim}}_{\text{ft,r,sc}} = N_{r,\text{sc}} \times P_{\text{ftu}} \times N_{\text{turns,r}} \times Y_{\text{rep}} \tag{2}$$

where, $N_{\text{r,sc}}$ is the number of ships per route and ship category, P_{fte} is the ship failure probability per hour (unique for each failure type), L_{r} is the length of the route (unit: metre), v_{sc} is the ship speed of the ship category (unit: metre/second), Y_{rep} is the number of repetitions of one year's traffic that the simulation set represents, P_{ftu} is the failure probability per turn (unique for the two failure types) and $N_{\text{turns,r}}$ is the number of turns per route. The probability of allision is then given by the number of simulated allisions divided by Y_{rep}.

Each simulation in all sets has a unique combination of values for the input parameters. This combination is generated in a Monte Carlo simulation using the distribution of each parameter. The input parameters that have distributions are those that control the simulated weather (wind, current and waves), ship set speed, heading and parameters related to the failure characteristics, such as the failure duration and angle deviations. As previously mentioned, the simulated ships are navigated by the autopilot and the implemented logic controlling the failure for a failure duration. If the ship strikes a ground or a bridge, the simulation is terminated early; otherwise, the simulation ends after the duration runs out. For further details on the STAPS methodology, see Hörteborn et al. [17].

2.2. Assessment of structural integrity consequences

The consequence assessment focuses on the energy involved in the structural integrity of the structures during a ship-bridge allision. The model originates from Minorsky [18] and Pedersen et al. [27], enabling a computationally efficient and sufficiently accurate model for a holistic assessment of ship-bridge allision risks. The approach considers the energy before and after the allision, i.e. how the striking ship's initial kinetic energy is distributed and dissipated into different energy terms and parts of the structures. The method is general and can be applied to fixed bridge structures (the pylons and the girder) or floating bridge structures (the bridge girder and the pontoons).

Since multiple models are used in the STAPS-cons methodology, three different coordinate systems are required. The MMS runs the ship simulation using a global coordinate system (X, Y). To determine the structural damage of a pontoon allision, a coordinate system relative to the pontoon orientation is used (turned γ_1, relative to X, Y coordinate system). Finally, to determine if it is a sliding or a head-on allision, a coordinate system relative to the surface is used (turned γ_2, relative to pontoon coordinate system). Fig. 3 illustrates these three coordinate systems with the angles β and α. The travel direction of the contact point of the ship is illustrated with a green arrow in the figure. However, the entire ship (not just the contact point) is modelled both in STAPS-cons and in the FE model.

The following equations present the general formulation for a bridge that may have floating structures. The initial kinetic energy of the ship before it strikes the bridge, K_0, is divided into eight components after the allision (similar to Wang et al. [37]) in Eq. (3).

$$K_0 = K_{\text{pos,ship}} + K_{\text{pos,bridge}} + W_{\text{hyd,ship}} + W_{\text{hyd,bridge}} + E_{\text{int,ship}} + E_{\text{int,bridge}} + W_{\text{fri}} \tag{3}$$

where K_{pos} refers to the remaining kinetic energy in the ship/bridge post-allision, W_{hyd} refers to the work done by hydrodynamic forces of the ship/bridge, E_{int} refers to the internal structural deformation energy in the ship/bridge and W_{fri} refers to the work done by friction forces. The kinetic energy of the ship is estimated using Eq. (4).

$$K_0 = \frac{(D_{\text{sc}} + A11_{\text{sc}}) \times u^2}{2} + \frac{(D_{\text{sc}} + A22_{\text{sc}}) \times v^2}{2} \tag{4}$$

In Eq. (4), D_{sc} is the displacement of the ship in ship category sc (unit: kg), $A11_{\text{sc}}$ is the added mass for the ship in its longitudinal direction, $A22_{\text{sc}}$ is the added mass in its lateral direction, u is the forward speed (unit: m/s) and v is the side speed (unit: m/s).

In oblique allisions, $K_{\text{pos,ship}}$ is estimated based on the Eurocode [5]. The Eurocode uses the terminology 'sliding impact', which is defined as a lateral impact angle (α) below 45°; see Fig. 3. The remaining kinetic energy in the ship for these allisions is estimated according to Eq. (5).

$$K_{\text{pos,ship}} = \begin{cases} K_0 \times cos(\alpha), & \alpha < 45 \\ 0, & \alpha \geq 45 \end{cases} \tag{5}$$

The remaining variables in Eq. (3) are estimated using nonlinear FEA for a few specific cases. Sha et al. [20] described this decoupled sequential local and global FEA simulation setup in detail. Further, the case study includes example cases and models from Jin et al. [38], although it builds on the FEA setup from Sha et al. [20]. The energy terms are taken directly from the FEA simulations at every timestep of the simulation.

For the local allision analysis, a Finite Element (FE) model was developed in LS-DYNA, including the striking ship's bow, the bridge's floating pontoon and the bridge deck. The FE model contains all major structural components, including the outer panels, decks, bulkheads, frames and stiffeners, using shell elements; see Fig. 4. It should be noted that this FE model accounts for both geometric and material nonlinearities.

During the simulation of the local FE model, the internal structural deformation energy ($E_{\text{int,ship}}$ and $E_{\text{int,bridge}}$) and the friction energy (W_{fri}) are estimated. Additionally, the local FEA simulation also generates a force-deformation curve, which is subsequently used in the global FEA simulation.

The global FE model is a generalised beam model representing the entire bridge's global structural stiffness. The global model is run after the local model where the energy is distributed between the bridge and the ship. Ye et al. [39] found that fluid-structure interaction can have an important effect on the global deformation of such a floating bridge. In this study, the hydrodynamic properties of the floating pontoons are based on the potential flow theory [23]. This theory was used to verify the accuracy of the Arbitrary Lagrangian-Eulerian (ALE) method. While the ALE method includes the effects of ship-generated waves, it is computationally intensive and time-consuming. The global floating bridge FE model is illustrated in Fig. 5.

In the global allision analysis, the kinetic energies of the ship and the bridge after allision ($K_{pos,ship}$ and $K_{pos,bridge}$) and the work done by hy-

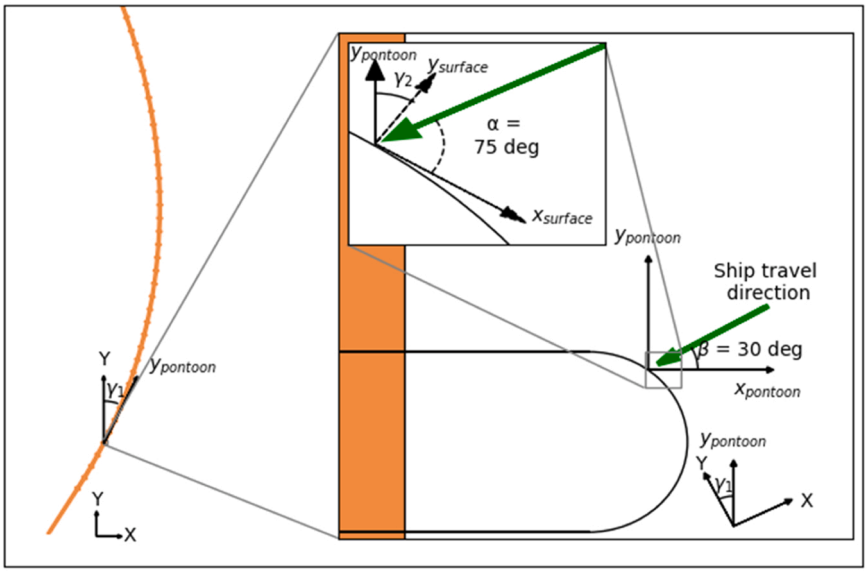

Fig. 3. The three coordinate systems used in STAPS-cons. The green arrow illustrates where the ship is travelling from. (X, Y) are used in the MMS model: $x_{pontoon}$, $y_{pontoon}$ is used to calculate the β angle for pontoon allisions and $x_{surface}$,$y_{surface}$ is used to calculate the α angle to determine sliding allisions.

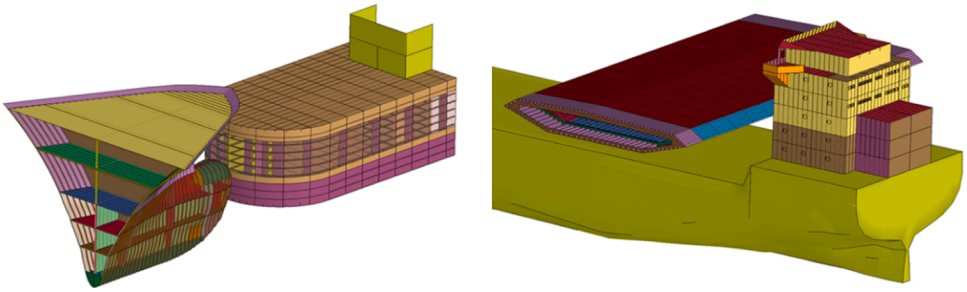

Fig. 4. The FE model of the ship and the pontoon (left) and the FE model of the ship deckhouse and bridge girder (right). The different colours represent different materials in the FE models.

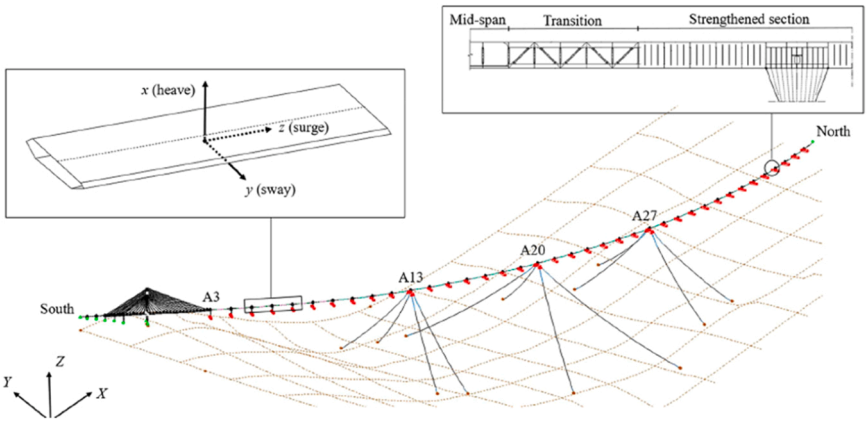

Fig. 5. Global finite element models used in the consequence analysis (figure from Wang et al. [23]).

drodynamic forces ($W_{hyd,\ ship}$ and $W_{hyd,\ bridge}$) are obtained. The local FEA simulation is run before the global FEA simulation since the bridge's natural period is long. While it would be ideal to include the global boundary condition in the local simulation, this refinement does not surpass the 'cost' with respect to model complexity and simulation time.

To summarise, the consequence is expressed as a scalar energy, derived from a sequence of coupled simulations and the initial kinetic energy obtained from MMS simulations. The distribution of energy between the local and the global structural components is based on nonlinear FEA results.

Finally, with all terms of Eq. (3) known, it is possible to review how many allisions occurred with a global or local energy greater than the structure's maximum capacity. The maximum capacity that the local part of the bridge can withstand is defined here as C_l (unit: MJ), and the maximum capacity that the global structure can withstand is defined here as C_g (unit: MJ). If these capacities are exceeded, the structure is

assumed to collapse. The total number of collapses (N_{col}) in Y_{rep} years can thereby be calculated by Eq. (6).

$$N_{col} = \sum_{i=1}^{no.allisions} \begin{cases} 1 & E_{int,bridge_i} > C_l or \left(K_{pos,bridge_i} + W_{hyd,bridge_i}\right) > C_g \\ 0 & Otherwise \end{cases} \tag{6}$$

3. Case study: Bjørnafjorden crossing

A case study using a real-world example demonstrates the capabilities of the STAPS-cons methodology. The case study focuses on the planned bridge over Bjørnafjorden, a fjord in the western part of Norway between Stavanger and Bergen. It is one of eight ferry crossings on the E39. The fjord is approximately 500 m deep and 5 kilometres wide at the planned fixed crossing location, which is being evaluated to reduce travel time. The weather is in this study represented by the current and the wind, which was obtained from local observations [43]. Westerly winds are dominant and wind from the north is rare in the area. However, the statistics for the ocean current reveals that northly current is the most common.

3.1. Bridge model

The planned bridge across Bjørnafjorden has a novel design; see Fig. 6 for an overview of its layout. Ship passage underneath the bridge is allowed in one location between a fixed pylon on the island of Svarvahelleholmen and a floating pontoon. The remaining spans of the bridge will not allow commercial ships to pass underneath due to insufficient free sailing height [40]. The 38 pontoons are identical with circular ends, a length of 50 m and a width of 15 m.

The bridge has been used in case studies presented by Jin et al. [38]. They simulated a variety of ship-allision scenarios and calculated the global allision energy $K_{pos,bridge} + W_{hyd,bridge}$ and the deformation energies $E_{int,ship}$ and $E_{int,bridge}$ in Eq. (3). Among others, they ran six simulations of ship-pontoon allisions: two with $\beta = 0°$, two with $\beta = 45°$ and two with $\beta = 90°$; see Fig. 7.

The relative distribution of energy in the six simulations illustrated in Fig. 7 is presented in Table 1. The energy is divided between global, local ship and local bridge in this table. The impact angle α is 45° or greater in all examples, and it is assumed that $K_{pos,ship}$ is 0 MJ in these allisions.

The percentages in Table 1 are approximate and based on these six FEA simulations, with a 160-metre-long container ship with a displacement of 20,000 tonnes at 8.2 m/s speed. However, the table is used for the division of energies for allisions regardless of ship category and ship speed. In future studies, it is recommended to investigate how this approximation affects the results of the analysis. Further, another assumption is that for the β angles between these three examples, the energy distribution could be linearly interpolated.

As indicated by Fig. 7, ships may hit the pontoon differently; the travel direction of the ship determines the β angle relative to the pontoon. However, two ships with similar β angles might have a large difference in the α angle (and vice versa). To give an example, two ships hit a pontoon with the same β angle, but they have different α angles. The first ship has an α angle of 90° and a β angle of 45°, which means that $K_0 \times 0.3$ of the ship's kinetic energy is transferred to the global bridge model, $K_0 \times 0.21$ is transferred to local ship deformation and $K_0 \times 0.49$ is transferred to local bridge deformation. In the second ship, the β angle is also 45°, but the α angle is 20°, making it a sliding allision. Eq. (5) is used to calculate $K_{pos,\ ship}$ and subtract it from the initial kinetic energy. This means that $K_0 \times (1 - \cos(\alpha)) \times 0.3$ of the energy is transferred to the global model, $K_0 \times (1 - \cos(\alpha)) \times 0.21$ is transferred to local ship deformation and $K_0 \times (1 - \cos(\alpha)) \times 0.49$ is transferred to local bridge deformation.

The bridge girder allisions have also been investigated by Jin et al. [38]. It was found that the bridge is stiffer closer to the shore compared to the centre of the bridge, as illustrated in Fig. 8. At these locations, three different ships with different speeds were simulated in LS-DYNA.

The relative distribution of energy in the simulations between the two locations illustrated in Fig. 8 is presented in Table 2. The energy is divided between bridge global, local ship and local bridge in this table. The impact angle α is 90°, and all the ship's kinetic energy is assumed to be consumed in the allision. It is assumed that the energy distribution of allisions between the mid-section and the end could be interpolated.

The actual structural integrity capacity of the bridge's design has not been finalised and will depend on the final selection of parameters, such as shell thickness. Yu et al. [41] and Storheim et al. [42] have conducted local FEA simulations with allisions at $\beta = 0°$ and K_0 up to 150 MJ. These simulations revealed that the pontoon experienced shell fractures at this energy level, which is used in this paper to set $C_l = 50$ MJ (using 30 % of 150 MJ according to Table 1). Storheim et al. [42] also performed global FEA simulations with K_0 up to 200 MJ, assuming that these occurred at mid-bridge and reached the global maximum capacity, resulting in C_g

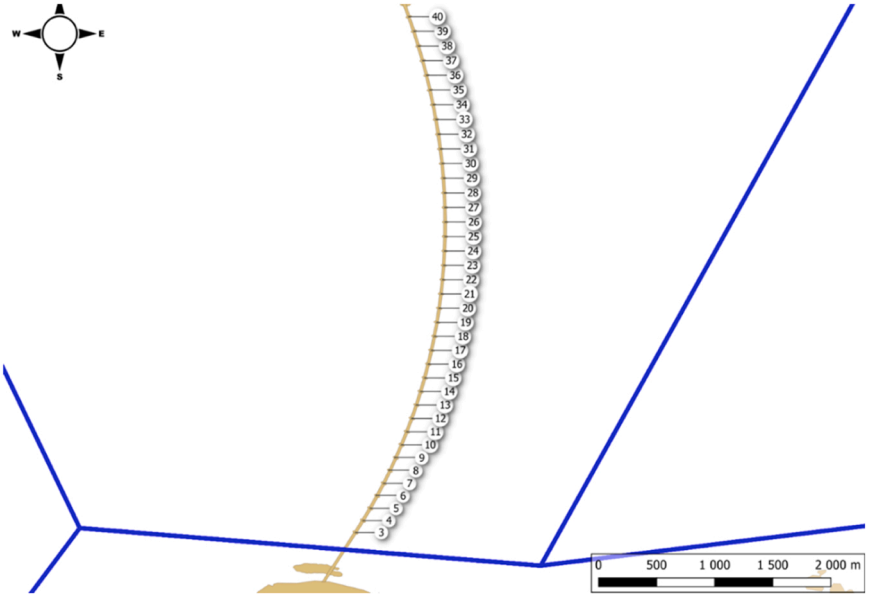

Fig. 6. Overview of the bridge layout, including the numbering of the pontoons. The blue lines indicate the simulation of future sailing routes.

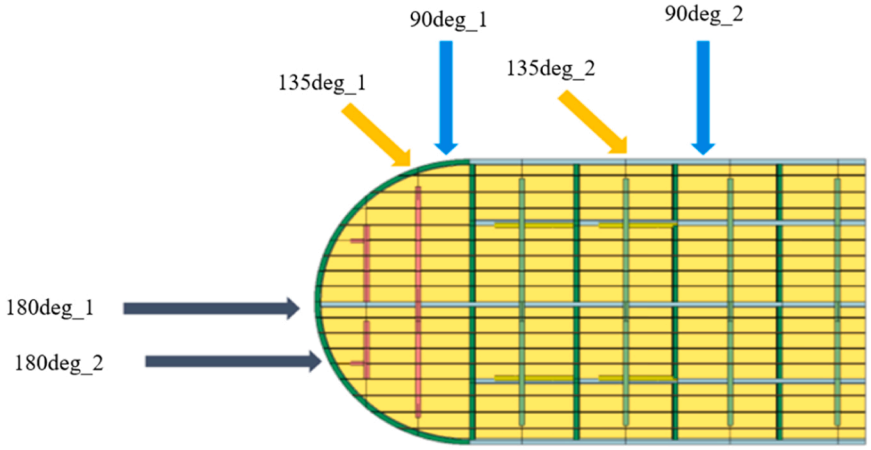

Fig. 7. LS-DYNA simulations of pontoon allisions in Jin et al. [38].

Table 1
Pontoon allision: percentages of the division of energies between the ship and the bridge. Figs. 3 and 7 contains the graphical interpretation of the angle β.

β	Bridge global energy ($K_{pos,bridge} + W_{hyd,bridge}$)	Local ship ($E_{int,ship}$)	Local bridge ($E_{int,bridge}$)
0, 180°: Transverse to bridge axis	50 %	20 %	30 %
45, 135, 225 and 315°	30 %	21 %	49 %
90, 270°: Parallel to bridge axis	10 %	18 %	72 %

Table 2
Distribution of energy in girder hits. *The mid bridge is considered the bridge girder around pontoon number 20; see Fig. 6.

	Bridge global energy ($K_{pos,bridge} + W_{hyd,bridge}$)	Local ship ($E_{int,ship}$)	Local bridge ($E_{int,bridge}$)
Impact close to one of the shores (Impl_2)	60 %	32 %	8 %
Impact at mid bridge* (Impl_1)	80 %	16 %	4 %

= 160 MJ (using 80 % of 200 MJ according to Table 2).

3.2. Ship traffic in the area

West of the inlet to the fjord, a busy ship route provides a sheltered path along the Norwegian west coast. Approximately 5600 passages were registered on this route during 2023, and almost 2000 ships passed into the Bjørnafjorden in the same year. For the final design, it is important to forecast how the ship sizes and number of ships will change in the future. Fig. 9 presents the AIS tracks from July 2023. It also shows four passage lines and the future ship routes. The four passage lines are used in the STAPS-cons methodology to count the number of ship passages and assign the number of ships on the routes.

The four passage lines I to IV in Fig. 9 were used to create the five ship traffic routes, lines 1–5, which define the ship traffic in two directions, resulting in 10 routes in total. A total of 1032 unique ships travelled on these routes in 2023 (excluding road ferries). These ships are categorised based on the ship type and ship size, into the seven ship categories presented in Table 3. The seven ship categories represent typical examples in the Bjørnafjorden area, and most vessels operate under similar loading conditions in both directions. However, the methodology allows for the inclusion of additional ship types and varying loading conditions in other case studies or geographic locations.

Each ship category was simulated with one MMS ship model with a

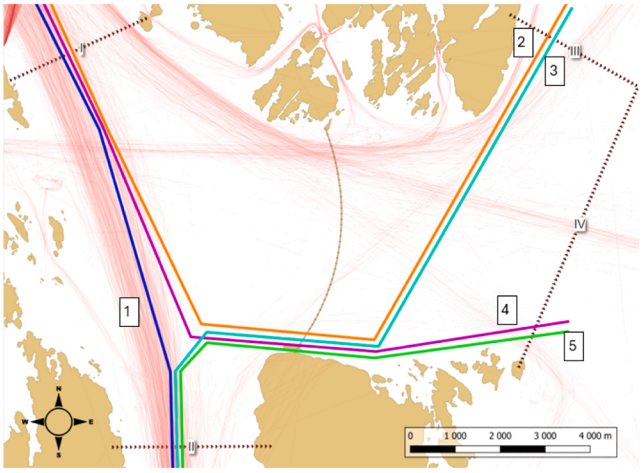

Fig. 9. Map over the Bjørnafjorden area with AIS data during July 2023 (excluding road ferries), the four passage lines (I-IV) and five future ship routes (1−5). Note: the lines are slightly offset in the figure from their intended positions to be visualised. Although the ship traffic varies in volume over the year, the pattern of how the ships navigate is rather constant. To reduce the number of lines in the figure, only the month of July was used.

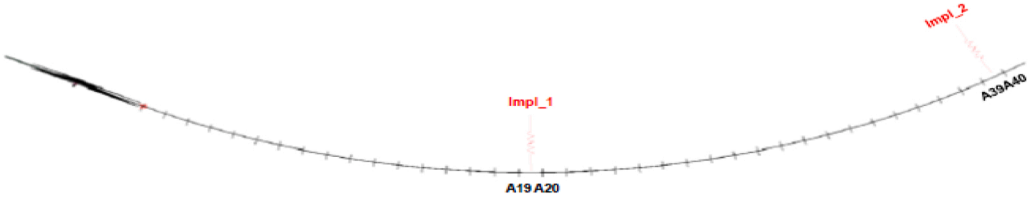

Fig. 8. Two different locations of impact from ship-bridge girder allisions.

Table 3
Overview of the ships included.

Ship category	Type	Length (m)	Deadweight (tonnes)
1	Product tanker	73	3200
2	Tanker	89	4850
3	General cargo	110	10,500
4	Military vessel	160	18,054
5	Container vessel	160	16,905
6	Tanker	160	27,600
7	Cruise ship	190	17,400

unique hydrodynamic and aerodynamic property. Ottosson [35] presented the main mathematical model in Seaman, which is the MMS used in this study. These seven ship types were simulated on all 10 routes to ensure that the autopilot had the capability to safely manoeuvre the ships from one end of the route to the other in various weather conditions. The AIS data also included the ship speed, which was used to generate a normal distribution for each combination of ship category and route. The number of ships in each ship category travelling on each route is presented in Table 4.

3.3. Failure probability and duration of failures

The STAPS-cons methodology requires the input of ship failure probabilities and their durations. A few scholars have conducted studies and presented examples of these values for specific geographic areas, waterways, and ship traffic conditions [32,44]. As no site-specific data for the Bjørnafjorden have been found, this case study adopted the values presented in Table 5, which were obtained by the authors in previous studies; see Hörteborn and Ringsberg [32] and Hörteborn and Eidem [33]. These values are assumed to be representative for the current case study since they are from a similar type of geography. However, in the final design of the structure, it is recommended to revisit these values and update them with site-specific probabilities and durations. Particular attention should be given to updating the durations associated with *Miss of turning point*, *WCT* and *TWL,* due to their strong correlation with location and the need to account for late discoveries (the "Heinrich factor" [45]).

3.4. Scenarios

The STAPS-cons methodology contains multiple input parameters. One of the main objectives of this study is to investigate how different input parameters, both related to probability and consequence estimations, could affect the risk of structural failure. There are numerous input parameters that could be altered, and an in-depth analysis of the area would be required to determine which parameters are most sensitive in each case and the range of the input values. The following scenarios are included to highlight the capabilities of the methodology:

1. Baseline
2. Increased probability of *miss of turning point* failure
3. Increased duration of *miss of turning point* failure
4. A less stiff structure, reduced energy uptake in the global model
5. A stiffer structure, increased energy uptake in the global model

Table 4
Number of ships travelling on each route.

Route	Ship 1	Ship 2	Ship 3	Ship 4	Ship 5	Ship 6	Ship 7
1	711	1124	434	35	7	208	287
2	810	1040	441	25	9	240	280
3	103	143	16	16	0	7	0
4	54	127	2	8	0	28	0
5	292	109	8	63	0	1	0
6	264	113	9	28	0	1	0
7	58	82	8	8	0	27	0
8	50	99	18	6	0	5	0
9	65	27	4	19	0	0	0
10	54	44	4	19	0	0	0

Table 5
Failure probabilities and duration used.

Failure type	Probability	Duration in seconds (μ, σ)
Loss of propulsion	0.65×10^{-4} per hour	Lognormal (6.63, 0.077)
Loss of steering	0.7×10^{-5} per hour	Lognormal (6.63, 0.077)
Miss of turning point	1.55×10^{-4} per turn	Normal (210, 60)
WCT	1.55×10^{-5} per turn	Lognormal (5.7, 0.45)
TWL	0.7×10^{-5} per hour	Lognormal (4.6, 0.4)

The baseline case used the failure probabilities given in Table 5 and the distribution of energies given in Tables 1 and 2. These values include likely modifications and regulations to the ship traffic that will be enforced when this bridge will be built, such as Traffic Separation Schemes (TSS) and Vessel Traffic Service (VTS).

Previous research [17,46] has highlighted that the probability and the duration of the failure *miss of turning point* are sensitive parameters in the probability estimation. These parameters could be affected by a lack of TSS and VTS. To see the sensitivity in these parameters, a 20 % increase in probability was investigated in Scenario 2 ($P_{\text{ft=miss of turning point}} = 1.2 \times 1.55 \times 10^{-4}$), and a 20 % increase in the duration of *miss of turning point* was assessed in Scenario 3 (Duration = Normal ($\mu = 210 \times 1.2$, $\sigma = 60 \times 1.2$)).

With regards to the consequence modelling, the impact of the stiffness of the structure was assessed in two scenarios. In Scenario 4, a less stiff bridge global model was used, and in Scenario 5, a stiffer bridge global model was used. These scenarios were evaluated using the percentages in Tables 6 and 7 instead of using the values in Tables 1 and 2. These values represented a 20 % decrease/increase in the amount of energy used by the global bridge. As the values were defined without any FEA simulations, they were included to illustrate the influence and importance of the FEA simulations in understanding how the ship's kinetic energy is distributed among local and global models.

4. Results

The 7600 ships per year in the area experience approximately 4.8 failures per year. To match the Norwegian design criterion in the Eurocode, Y_{rep} was set to 10^6 (repeating the failures one million times) [6], which results in 4.8 million failure simulations to run in the MMS. The majority of these failures will result in the failure/error being resolved or in grounding accidents. However, some will also hit the bridge. The number of simulations and allisions is presented separately per failure type in Table 8. The paths of the ships that were simulated with allisions are illustrated in Fig. 10.

The data from the allisions were post-processed, and the allision energy was split into the components of Eq. (3). Each allision in this case study has a probability of occurring of 1×10^{-6} per year (since the traffic was defined per year, and Y_{rep} was set to 10^6 repetitions of the year). To pass the Norwegian criterion [6], the number of allisions

Table 6
Distribution of energy in the scenarios with a [less stiff, stiffer] global model for pontoon hits.

	Bridge global energy ($K_{\text{pos,bridge}} + W_{\text{hyd,bridge}}$)	Local ship ($E_{\text{int,ship}}$)	Local bridge ($E_{\text{int,bridge}}$)
0°: Transverse to bridge axis	[40 %, 60 %]	[24 %, 16 %]	[36 %, 24 %]
45°	[24 %, 36 %]	[23 %, 19 %]	[53 %, 45 %]
90°: Parallel to bridge axis	[8 %, 12 %]	[19 %, 19 %]	[73 %, 69 %]

Table 7
Distribution of energy in the scenarios with a [less stiff, stiffer] global model for girder hits.

	Bridge global energy ($K_{pos,bridge} + W_{hyd,bridge}$)	Local ship ($E_{int,ship}$)	Local bridge ($E_{int,bridge}$)
Impact close to shore	[48 %, 72 %]	[41 %, 23 %]	[11 %, 5 %]
Impact mid bridge	[64 %, 96 %]	[28 %, 3 %]	[8 %, 1 %]

Table 8
Number of simulations and allisions based on the yearly failure rates and $Y_{rep} = 10^6$.

	Number of simulations	Number of allisions
Loss of propulsion	455,904	420
Loss of steering	49,071	160
Miss of turning point	3860,892	109
WCT	386,045	247
TWL	49,071	71
Total	4800,983	1007

causing structural collapse, N_{col}, must be less than 100 (which will add up to a probability of 1×10^{-4} per year).

With regards to the consequences of the allisions, Fig. 11 illustrates that most of the pontoon allisions occurred with a β angle between 22.5° and 67.5°, and that allisions with a β angle above 67.5° were rare. Furthermore, the figure also illustrates that most of the allisions are considered sliding allisions.

4.1. Results of the sensitivity scenarios

The results from the five scenarios are presented in this subchapter and compared in the next subchapter. In Scenario 1 (the baseline case), with C_l set to 50 MJ and C_g set to 160 MJ, in accordance with [41,42], the simulations found 81 allisions where the maximum energy was above the structure's maximum energy, equal to a bridge collapse probability of 0.81×10^{-4} per year. To give two examples of allisions causing collapses:

- 162 MJ in global energy corresponding with a military ship with a deadweight of 18,000 tonnes at 16 knots hitting the bridge girder close to the north end with an $\alpha = 50°$.
- 56 MJ in local energy corresponding with the military ship at 11 knots hitting a pontoon with an $\alpha = 60°$ and a $\beta = 43°$.

However, C_l and C_g could be changed with a detailed design (for example, increased/decreased shell thickness). How this affects N_{col} in the baseline is illustrated as a 3D surface in Fig. 12.

The flat surface in Fig. 12, with a design where $C_l > 150$ MJ and $C_g > 200$ MJ, illustrates that there were zero allisions leading to structural collapse with this design (probability of collapse $<1 \times 10^{-6}$). The colour of the surface indicates the distribution of allisions that surpassed C_g, i.e. with a $C_l > 150$ MJ; all structural collapses were caused by allisions with a $W_{hyd,bridge}+E_{bridge}>C_g$.

The design criterion of one structural collapse in 10^4 years is illustrated by the black line. This indicates how C_l and C_g could be varied to maintain $N_{col} = 100$; this line is further discussed and analysed in Fig. 15.

Scenarios 2 and 3 involved an increased probability and duration of the miss of the turning point failure, leading to a different set of simulations and allisions, presented in Table 9. Specifically, Scenario 2 required a 20 % increase in the number of simulations compared to Scenario 1 and an increase in the number of allisions. The number of simulations in Scenario 3 remained the same as in Scenario 1; hence the number of allisions drastically increased. Scenarios 4 and 5 maintained the same number of simulations and allisions as Scenario 1.

The number of allisions caused by *miss of turning point* increased from 109 to 136 when the probability increased by 20 %, resulting in a slightly more than 20 % increase. This is due to the randomness in the output from the Monte Carlo simulation for the input parameters. With the 20 % increase in the duration of *miss of turning point,* the number of allisions caused by the failure increased from 109 to 500. Further analysis, with C_l set to 50 MJ and C_g set to 160 MJ, reveals that N_{col} in Scenario 2 became 78 and 166 in Scenario 3. How the N_{col} varies for these scenarios with varying C_l and C_g is illustrated in Fig. 13.

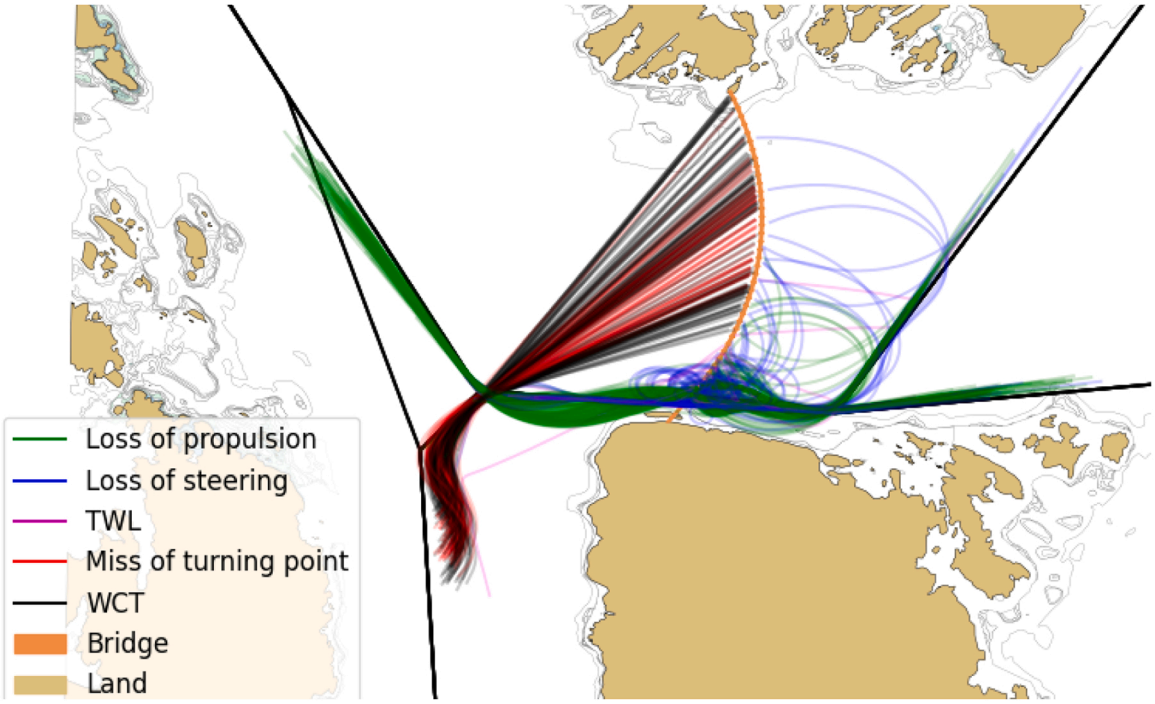

Fig. 10. Overview of the 1007 ship paths that struck the bridge.

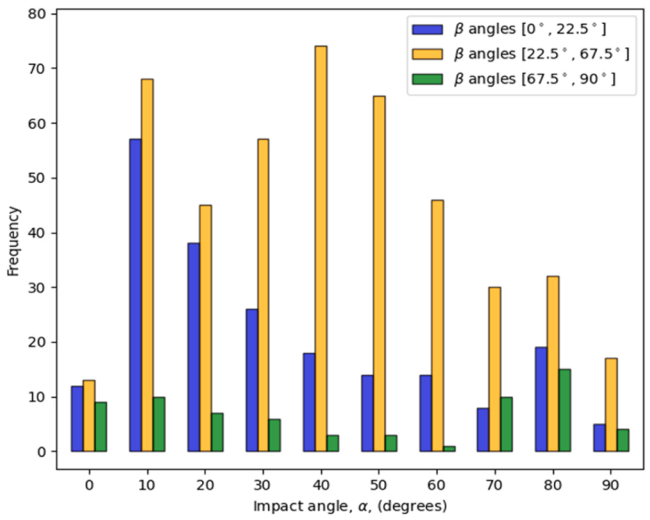

Fig. 11. Distributions of α angles for the allisions with different groups of β angles.

The increased probability of the *miss of turning point* failure in Scenario 2 gave a similar result to the baseline in Scenario 1. However, the increased duration in Scenario 3 had a larger effect on the results. This is illustrated in Fig. 13 with a higher number of N_{col} for Scenario 3 compared to Scenario 2.

To evaluate Scenarios 4 and 5, the allisions from the baseline in Scenario 1 were used, combined with Tables 6 and 7 (instead of Tables 1 and 2). This resulted in $N_{col} = 67$ for Scenario 4, using the less stiff global model, and $N_{col} = 113$ for Scenario 5, using the stiffer global model. How the N_{col} varies for these scenarios with varying C_l and C_g is illustrated in Fig. 14.

The colours in Fig. 14 illustrate that the stiffness of the global model has a major impact on the cause of the structural failure. Using the less stiff global model increases the N_{col} caused by $E_{int,bridge} > C_l$, while the stiffer global model increases the N_{col} caused by $W_{hyd,bridge} + E_{bridge} > C_g$. This is expected since less of the total energy is transferred into global energy with the less stiff global model and vice versa with the stiffer model that had more of the total energy transferred to the global model.

4.2. Comparison of the different scenarios

A summary of the results from the five scenarios with C_l set to 50 MJ and C_g set to 160 MJ is presented in Table 10. The probability of collapse is under the Norwegian criterion in Scenarios 1, 2 and 4.

To compare the parameters' influence on the result, the lines where $N_{col} = 100$ in Figs. 12, 13 and 14 could be compared; see Fig. 15. The lines should be regarded as the minimum combination of C_l and C_g to meet the 10^{-4} criterion.

The black solid line in Fig. 15 indicates that Scenario 1 (the baseline case) requires at least 120 MJ in C_g (if C_l is at least 125 MJ), and vice versa, C_l needs to be at least 20 MJ (if C_g is at least 180 MJ). This figure can thereby be used to find the balance between the required local and global design.

The example values of C_l and C_g are included in Fig. 15. Scenarios 1, 2 and 4 are constantly to the left/below these lines and, thereby, the probability of collapse is less than 1×10^{-4} per year. However, Scenarios 3 and 5 are partly to the right/above these lines and, thereby, have a probability of collapse greater than 1×10^{-4} per year. It is important to highlight that this figure represents $N_{col} = 100$ and does not provide any information on how many allisions would collapse the bridge 'outside' of these lines.

Even though Scenario 2 included more allisions caused by *miss of turning point* compared to Scenario 1 (136 compared to 109), the number of collapses was slightly lower (78 compared to 81). This was not expected but could be explained with Fig. 15, specifically where the red/black lines cross the orange lines. Both the black and the red lines cross the 50 MJ local C_l at 145 MJ in global C_g. However, just around 160 MJ for C_g, there is a slight 'drop' in the red curve compared to the black, which explains the drop of N_{col} from 81 to 78. Zooming out from the C_l and C_g criteria, the red line is right of the black line for C_l greater than 60 MJ, which indicates that more of the allisions in Scenario 2 (compared to Scenario 1) caused greater local damage rather than global damage.

Scenarios 4 and 5, with C_l above 50 MJ, illustrate that the amount of energy consumed by the global deformation (see Table 1 vs. Table 6) almost has a linear effect on how much energy is required for C_g.

Table 9
Number of simulations where the probability and duration were increased by 20 % in two separate case studies.

	Number of simulations		Number of allisions	
	Scenario 2	Scenario 3	Scenario 2	Scenario 3
Loss of propulsion	455,904	455,904	420	419
Loss of steering	49,071	49,071	160	159
Miss of turning point	4633,066	3860,892	136	500
WCT	386,045	386,045	247	148
TWL	49,071	49,071	71	70
Total	5573,157	4800,983	1035	1398

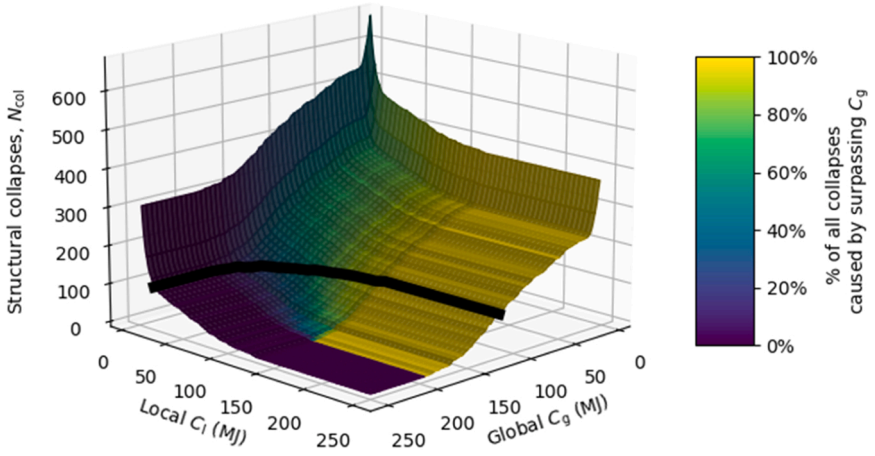

Fig. 12. Number of collapses, N_{col}, as a 3D surface in the baseline, depending on the design of C_l and C_g. The black line represents where the surface overlaps with the Norweigan criterion (1 structural failure every 10^4 years).

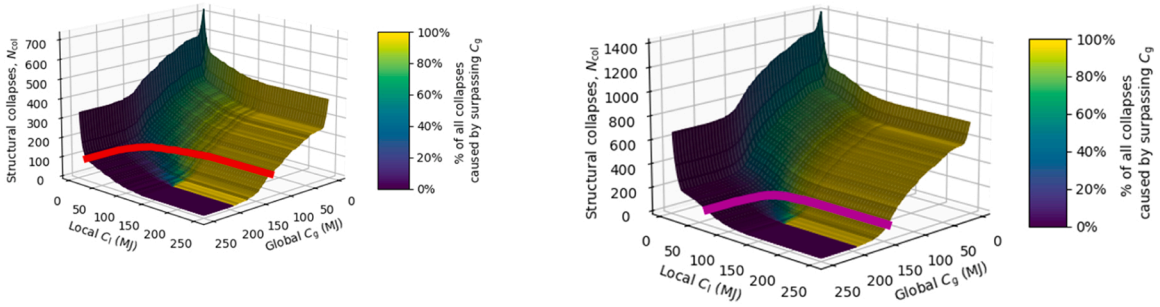

Fig. 13. N_{col} as a 3D-surface depending on the design of C_l and C_g, using Scenario 2 (left) and Scenario 3 (right). The red line (Scenario 2) and the magenta line (Scenario 3) represent where the surface overlaps with the Norwegian criterion (1 structural failure every 10^4 years).

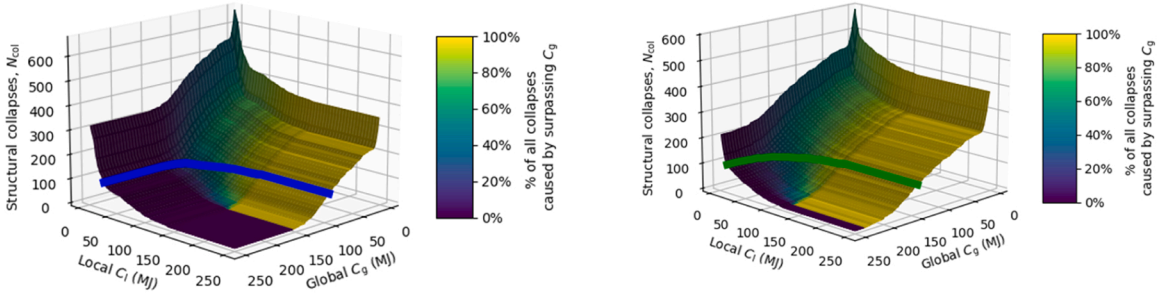

Fig. 14. N_{col} as a 3D-surface depending on the design of C_l and C_g, using Scenario 4 (left) and Scenario 5 (right). The blue line (Scenario 4) and the green line (Scenario 5) represent where the surface overlaps with the Norwegian criterion (1 structural failure every 10^4 years).

Table 10
The probability of collapse (N_{col}/Y_{rep}) with C_l set to 50 MJ and C_g set to 160 MJ.

	Scenario 1	Scenario 2	Scenario 3	Scenario 4	Scenario 5
Probability of collapse	0.81 × 10–4	0.78 × 10–4	1.66 × 10–4	0.67 × 10–4	1.13 × 10–4

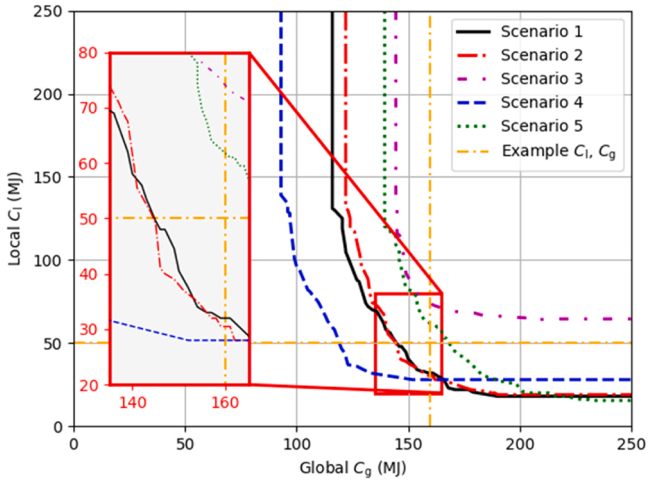

Fig. 15. The combination of minimum strength with the regards to local and global strength, for a failure rate of 10^{-4}.

Scenario 4, with the less stiff global model, has a lower requirement for C_g compared to the other scenarios; however, this scenario has a larger requirement for C_l.

5. Discussion

In this paper, a methodology for assessing the risk of ship-bridge allisions has been described. Pedersen et al. [27] and others have conducted similar studies, where one model has been used to assess the probability and another model to assess the consequence of allisions. However, the STAPS-cons methodology described in this paper assesses the risk of collapse due to ship-bridge allisions in a unified approach, without separating the analysis of probability and consequence into different models. While Pedersen's framework [27] and related studies have contributed significantly to the understanding of ship–bridge allision mechanics, they typically treat probability and consequence as separate analytical domains. In contrast, the STAPS-cons methodology integrates these aspects into a unified simulation framework, enabling simultaneous assessment of failure likelihood and structural impact. This integration not only streamlines the risk evaluation process but also enhances the fidelity of scenario-based assessments. The originality of STAPS-cons lies in its capacity to couple probabilistic ship manoeuvre simulations with nonlinear finite element consequence modelling, thereby overcoming the fragmentation inherent in previous approaches. This holistic methodology allows for a more thorough understanding of ship-bridge allisions, considering both the mechanical properties of the structures and the dynamic behaviours of ships.

As demonstrated, it is possible to use the proposed methodology to assess different options regarding the local and global strength of the structure. However, the results of the case study show that the STAPS-cons methodology is sensitive to both the parameters related to the allision probability estimation and the estimation of kinetic energy. Reducing the amount of kinetic energy that the global model absorbs with a less stiff global model reduced the demand on the structure; however, the manners in which the stiffness can be reduced was not studied here. As previous research has also identified, the duration of the failure type *miss of turning point* is a crucial parameter. Hörteborn et al. [17] illustrated why this parameter might have an exponential impact in addition to why a 20 % increase in this duration led to a dramatic

increase in the number of allisions and an increased need for structural strength.

The unexpected results when comparing Scenarios 1 and 2, with C_l set to 50 MJ and C_g set to 160 MJ, indicate that the random influence of the Monte Carlo simulation was greater than the 20 % increase in the failure *probability of miss of turning point*. In Hörteborn et al. [17] the number of allisions using the same input with a different random seed was analysed. If the number of allisions differed by more than 5 %, Y_{rep} needed to be increased. Future research should recommend similar criteria with respect to the number of collapses.

The included scenarios highlight the importance of obtain inputs for probability estimation and outputs from FEA simulations that are as precise as possible when conducting a risk assessment. FEA simulations are crucial in describing how the kinetic energy from a ship is distributed in an allision. However, as previously highlighted there was only one ship type hitting the pontoon at one speed in a limited number of locations in the FEA simulations. Further studies are recommended to investigate this in more detail to determine a minimum number of FEA simulations. Regarding the probability assessment, there are many more parameters that are important to analyse, for example, the expected vessel traffic (how many ships of different sizes, their speeds and their distribution over the fairway) and the local failure probability and duration.

Assessing mitigation options is a crucial part of risk assessment to reduce the risk of allisions. Specific risk mitigation options have not been exemplified in this study; however, the scenarios could represent different options. These options can target minimising the probability or consequences of the incident [47]. Other general actions include reducing the probability of allisions through the addition of VTS [32,48] and changing the route layout [32]. To mitigate the consequence of allisions, the structure could be designed to withstand allisions with higher energies [49,50]; similarly protective structures could be added to protect the bridge pillars [51–54]. Chen et al. [55] proposed the use of an adaptive arresting vessel device, which might completely stop some vessels or at least reduce their speed. However, the effect of these mitigations could be difficult to compare by using one tool to assess the probability and another to assess the consequences. Therefore, there is a need for the STAPS methodology to include both the probability and the consequences of an allision.

The complexity and the number of components involved in the proposed methodology might limit its usage. For example, failure modelling requires a substantial quantity of AIS data to find local failure statistics and a ship simulator capable of running manoeuvre simulations in fast-time mode. In addition, non-linear FEA computations require a high level of expertise to set up and significant resources to run. However, in relation to the cost of building and maintaining these large bridges, the cost of using the proposed methodology is small. Further, reducing the uncertainty in the risk assessment with a methodology capable of assessing uncertainties in different types of input could reduce building costs. Also, as addressed by Wu et al. [56], as the bridge ages, the material strength decreases, and detailed assessments of a specific allision might be less relevant to the design criteria.

One of the main strengths of this methodology is its capability to address risk mitigation options related to both navigation and the structure itself. The methodology can, for example, evaluate navigational restrictions, the width of the bridge span (navigational span), and the structural strength all within one methodology. This adds the possibility of addressing different stakeholders' interests in a comprehensive manner.

6. Conclusions

This study presented the development and application of the STAPS-cons methodology, a unified approach for assessing the risk of ship-bridge allisions by integrating both probability and consequence assessments. This integrated approach provides a comprehensive risk assessment where the same tool is used to analyse both the probability and the consequences of an allision.

One of the main strengths of the STAPS-cons methodology is its ability to evaluate the risk of bridge collapse and assess the influence of options related to both navigation and structural design. This capability allows for a holistic assessment of different stakeholders' interests, facilitating more informed decision-making. While the methodology's complexity poses challenges, such as the need for AIS data and advanced simulation tools, it also reduces uncertainty in risk assessments by addressing multiple uncertainties within a single methodology. Future research should focus on improving the accuracy of different models within the methodology, exploring new risk mitigation strategies and extending the methodology to other types of structures and accidents. A promising avenue for further development is the integration of dynamic consequence modelling through embedded FEA simulations, which could enhance impact accuracy but also introduce considerable computational demands. Moreover, external validation using historical allision data would help strengthen the credibility and practical relevance of the methodology. The practical implications of this research are significant for bridge designers, policymakers and maritime authorities.

However, the case study demonstrates that the developed methodology is sensitive to the parameters that affect both the probability and the consequences of an allision. Notably, the STAPS-cons model uses the distribution between global bridge, local bridge and local ship of the initial kinetic energy from FEA simulations, resulting in a linear influence on the required structural strength to withstand allisions. The study highlights the critical role of the duration of failures, such as the miss of turning point, in determining the risk of collapse. A 20 % increase in failure duration led to a substantial increase in the number of allisions and a corresponding need for a stronger bridge, making this a vital parameter to consider in this methodology.

In conclusion, the STAPS-cons methodology represents a significant advancement in the field of ship-bridge allision risk assessment. Of the five scenarios analysed in this paper, three passed and two failed the Norwegian criterion for the probability of collapse, which is less than 10^{-4} per year. By integrating probability and consequence assessments, this methodology offers a more robust and comprehensive tool for managing the risks associated with increased shipping traffic and bridge construction in navigational waters.

CRediT authorship contribution statement

Ringsberg Jonas: Writing – review & editing, Writing – original draft, Supervision, Project administration, Methodology, Conceptualization. **Olov Lundbäck:** Writing – review & editing, Supervision, Software, Conceptualization. **Wengang Mao:** Writing – review & editing, Supervision, Project administration. **Yanyan Sha:** Writing – original draft, Validation, Software, Formal analysis, Data curation, Conceptualization. **Axel Hörteborn:** Writing – review & editing, Writing – original draft, Visualization, Software, Methodology, Funding acquisition, Formal analysis, Conceptualization.

Declaration of Generative AI and AI-assisted technologies in the writing process

During the preparation of this work the author(s) used Microsoft Copilot in order to check the grammar of the text. After using this tool/service, the author(s) reviewed and edited the content as needed and take(s) full responsibility for the content of the publication.

Declaration of Competing Interest

The authors declare the following financial interests/personal relationships which may be considered as potential competing interests: Axel Hörteborn reports financial support was provided by Swedish Transport Administration. Axel Hörteborn reports financial support was

provided by Norwegian Public Roads Administration. Axel Hörteborn reports financial support was provided by Research Institute of Sweden. Jonas Ringsberg reports financial support was provided by Norwegian Public Roads Administration. Wengang Mao reports financial support was provided by Norwegian Public Roads Administration. Yanyan Sha reports financial support was provided by Norwegian Public Roads Administration. If there are other authors, they declare that they have no known competing financial interests or personal relationships that could have appeared to influence the work reported in this paper.

Acknowledgement

This research has been funded by the Norwegian Public Road Administration, the Swedish Transport Administration and RISE (Research Institutes of Sweden).

Data availability

Data will be made available on request.

References

[1] NTSB. Contact of containership dali with the Francis Scott key bridge and subsequent bridge collapse. 2024.
[2] Zhang WZ, Pan J, Sanchez JC, Li XB, Xu MC. Review on the protective technologies of bridge against vessel collision. Thin Walled Struct 2024;201:112013. https://doi.org/10.1016/j.tws.2024.112013.
[3] UNCTAD. Review of Maritime Transport 2024. Geneva: United Nations Publications; 2024.
[4] AASHTO. Guide specifications and commentary for vessel collision design of highway bridges. 2nd edition. U.S.: American Association of State Highway and Transportation Officials (AASHTO); 2009.
[5] CEN. Eurocode 1: Actions on structures - Part 1-7: General actions - Accidental actions. Brussels, Belgium: European Committee for Standardization; 2006.
[6] Statens Vegvesen. Håndbok N400 Bruprosjektering - Eurokodeutgave. Håndbok N400 Bruprosjektering - Eurokodeutgave, Statens Vegvesen; 2014..
[7] Ćorić M, Mandžuka S, Gudelj A, Lušić Z. Quantitative ship collision frequency estimation models: a review. J Mar Sci Eng 2021;9:533.
[8] Xiao F, Ma Y, Wu B. Review of probabilistic risk assessment models for ship collisions with structures. Appl Sci 2022;12:3441. https://doi.org/10.3390/app12073441.
[9] Galić S, Lušić Z, Mladenović S, Gudelj A. A chronological overview of scientific research on ship grounding frequency estimation models. JMSE 2022;10:207. https://doi.org/10.3390/jmse10020207.
[10] Fujii Y, Yamanouchi Oshima R, Mizuki H. N. Some factors affecting the frequency of accidents in marine traffic: I-the diameter of evasion for crossing encounters, II-the probability of stranding, III-the effect of darkness of the probability of collision and stranding. J Navig 1974;27:239–47.
[11] Macduff T. The probability of vessel collisions. Ocean Ind 1974;9:144–8.
[12] Pedersen PT. Collision and grounding mechanics, 1. Copenhagen, Denmark: Danish Society of Naval Architecture and Marine Engineering; 1995. p. 125–57.
[13] Friis-Hansen P. Basic modelling principles for prediction of collision and grounding frequencies. 2008.
[14] Engberg P.C. IWRAP Mk2 v5.3.0 manual. GateHouse A/S, IALA; 2017.
[15] IMO. Degree of Risk Evaluation. London: IMO; 2010.
[16] Bąk A, Gucma S, Przywarty M. Models of Navigation Risk Used in Restricted Areas. Safety of Navigation in Restricted Areas: Methods of Risk Estimation and Analysis. Cham: Springer Nature Switzerland; 2024. p. 57–97. https://doi.org/10.1007/978-3-031-49532-8_2.
[17] Hörteborn A, Ringsberg JW, Wengang M, Lundbäck O. Probabilistic analysis of ship-bridge allisions when designing bridges. Reliab Eng Syst Saf 2025;260. https://doi.org/10.1016/j.ress.2025.111026.
[18] Minorsky VU. An analysis of ship collisions with reference to protection of nuclear power plants. New York: Sharp (George G.) Inc.; 1958.
[19] Le Sourne H, Besnard N, Cheylan C, Buannic N. A ship collision analysis program based on upper bound solutions and coupled with a large rotational ship movement analysis tool. J Appl Math 2012;2012:375686.
[20] Sha Y, Amdahl J, Dørum C. Local and global responses of a floating bridge under ship–girder collisions. J Offshore Mech Arct Eng 2019;141. https://doi.org/10.1115/1.4041992.
[21] Chen TL, Cheng YH, Wu H. A simplified simulation strategy for barge-bridge collision learned from collapse of Taiyangbu Bridge. Eng Struct 2024;303:117592. https://doi.org/10.1016/j.engstruct.2024.117592.
[22] Lu WJ, Zhang LM, Liu HT, Cai SW. Energy analysis of progressive collapses in a multi-span bridge under vessel impact using centrifuge modelling. Eng Struct 2022;266:114591. https://doi.org/10.1016/j.engstruct.2022.114591.
[23] Wang Z, Sha Y, Jakobsen JB. Floating bridge response under combined ship collision, wind and wave loads. Ships Offshore Struct 2023:1–18. https://doi.org/10.1080/17445302.2023.2195242.
[24] Petersen M.J., Pedersen P.T. Collisions Between Ships and Offshore Platforms, 1981, p. OTC-4134-MS. https://doi.org/10.4043/4134-MS.
[25] Pedersen PT, Valsgård S, Olsen D, Spangenberg S. Ship impacts: Bow collisions. Int J Impact Eng 1993;13:163–87. https://doi.org/10.1016/0734-743X(93)90091-K.
[26] Pedersen P.T., Jensen J.J. Ship impact analysis for bottom supported offshore structures. 1991.
[27] Pedersen PT, Chen J, Zhu L. Design of bridges against ship collisions. Mar Struct 2020;74:102810. https://doi.org/10.1016/j.marstruc.2020.102810.
[28] Pedersen PT, Zhang S. On impact mechanics in ship collisions. Mar Struct 1998;11:429–49.
[29] Zhang S, Villavicencio R, Zhu L, Pedersen PT. Impact mechanics of ship collisions and validations with experimental results. Mar Struct 2017;52:69–81.
[30] Zhang S, Pedersen PT, Villavicencio R. of ship collision and grounding. Butterworth-Heinemann. Probab Mech 2019.
[31] Pedersen PT. Review and application of ship collision and grounding analysis procedures. Mar Struct 2010;23:241–62. https://doi.org/10.1016/j.marstruc.2010.05.001.
[32] Hörteborn A, Ringsberg JW. A method for risk analysis of ship collisions with stationary infrastructure using AIS data and a ship manoeuvring simulator. Ocean Eng 2021;235:109396. https://doi.org/10.1016/j.oceaneng.2021.109396.
[33] Hörteborn A., Eidem M.E. Probability of active navigational failure. Journal of Navigation 2025; Accepted. https://doi.org/10.1017/S0373463325101100, (available 2025-08-14).
[34] RISE. SEAMAN simulations 2020. https://www.ri.se/en/expertise-areas/test-demo/seaman-simulations (accessed May 19, 2025)..
[35] Ottosson P. Mathematical models in PORTSIM. Mathematical models in PORTSIM, Southampton, UK: 1994.
[36] sspasweden. PySim. Github 2020. https://github.com/sspasweden/pysim (accessed May 19, 2025)..
[37] Wang Z., Sha Y., Jakobsen J.B. Coupled Analysis of External Dynamics and Internal Mechanics in Ship-Floating Bridge Collision Studies. OMAE2024, Volume 2: Structures, Safety, and Reliability: 2024. https://doi.org/10.1115/OMAE2024-123345.
[38] Jin Y, Sha Y, Moan T. Risk Analysis of a floating bridge subjected to ship collisions. Trondheim, Norway: NTNU for Norwegian Public Road Administration; 2020.
[39] Ye X, Fan W, Sha Y, Hua X, Wu Q, Ren Y. Fluid-structure interaction analysis of oblique ship-bridge collisions. Eng Struct 2023;274:115129. https://doi.org/10.1016/j.engstruct.2022.115129.
[40] Statens Vegvesen. SBJ-33-C5-OON-22-RE-100–0 K12 - Fjordcrossing Björnafjorden. 2019..
[41] Yu Z, Wang X, Moan T, Amdahl J, Sha Y. Ultimate and residual strength assessments of intact and collision damaged columns of the Bjørnafjorden floating bridge. Advances in the Collision and Grounding of Ships and Offshore Structures. CRC Press; 2023. p. 387–93.
[42] Storheim M, Jakobsen SE, Nedrebø ØK. Preferred solution, K12 – Appendix J Ship collision. Statens Vegvesen; 2019.
[43] Knutsen Ø, Stefanakos C. Ferry-free E39 - Currents. Trondheim, Norway: Sintef ocean; 2022.
[44] Rasmussen FM, Glibbery KAK, Melchild K, Hansen MG, Jensen TK, Lehn-Schiøler T, et al. Quantitative assessment of risk to ship traffic in the Fehmarnbelt fixed link project. J Pol Saf Reliab Assoc 2012;3:1–12.
[45] Heinrich HW. Industrial Accident Prevention. A Scientific Approach. New York & London: McGraw-Hill Book Company, Inc; 1941.
[46] Ylitalo J. Modelling Marine Accident Frequency. Espoo: Aalto University; 2010.
[47] Aven T, Krohn BS. A new perspective on how to understand, assess and manage risk and the unforeseen. Reliab Eng Syst Saf 2014;121:1–10. https://doi.org/10.1016/j.ress.2013.07.005.
[48] Lehn-Schiøler T, Hansen MG, Melchild K, Jensen TK, Randrup-Thomsen S, Glibbery KAK, et al. VTS a risk reducer: a quantitative study of the effect of VTS Great Belt. Collision and Grounding of Ships and Offshore Structures. CRC Press/Taylor and Francis Group, London; 2013. p. 19–26.
[49] Fan W, Shen D, Huang X, Sun Y. Reinforced concrete bridge structures under barge impacts: FE modeling, dynamic behaviors, and UHPFRC-based strengthening. Ocean Eng 2020;216:108116. https://doi.org/10.1016/j.oceaneng.2020.108116.
[50] Sha Y, Amdahl J, Yang K. An efficient approach for ship collision design of reinforced concrete pontoon walls. IOP Publ 2019;700:012038.
[51] Zhao S, Fang H, Wang R, Cao P. Ship collision performance of a fiber-reinforced composite material winding tube filled with ceramic pellets. Eng Struct 2025;324:119335. https://doi.org/10.1016/j.engstruct.2024.119335.
[52] Zhou S, Fang H, Zhang X, Zhu L, Wang S. Ship collision performance of a flexible anti-collision device designed with fiber-reinforced rubber composites. Eng Struct 2024;302:117472. https://doi.org/10.1016/j.engstruct.2024.117472.
[53] Yang J, Ban D, Shi J. Experimental and numerical investigations of a novel steel-UHPC-polyurethane composite fender against vessel collisions. Eng Struct 2025;330:119911. https://doi.org/10.1016/j.engstruct.2025.119911.
[54] Cheng Y, Wang W, Zhou C, Guo K, Liang L, Zhao Q. A novel steel-GFRP-foam composite fender for reinforced concrete pier protection subjected to vessel collision. Eng Struct 2025;330:119938. https://doi.org/10.1016/j.engstruct.2025.119938.
[55] Chen, Wang W, W.Li YG, Yang LM, Liu J, Dong XL, et al. An adaptive arresting vessel device for protecting bridges over non-navigable water against vessel collision. Eng Struct 2021;237:112145. https://doi.org/10.1016/j.engstruct.2021.112145.
[56] Wu H, Liu X, Cheng YH, Chen TL. Dynamic behaviors of bridge with corroded RC piers under barge collisions. Eng Struct 2024;319:118843. https://doi.org/10.1016/j.engstruct.2024.118843.